International Journal of Medical, Medicine and Health Sciences
ISSN: 2517-9969
Vol:5, No:7, 2011

Pro-inflammatory Phenotype of COPD Fibroblasts not Compatible with Repair in COPD Lung

Jing Zhang[1], Lian Wu[2*], Jie-ming Qu[3], Chun-xue Bai[1], Mervyn J Merrilees[4], Peter N Black[2]

***Abstract*—**COPD is characterized by loss of elastic fibers from small airways and alveolar walls, with the decrease in elastin increasing with disease severity. It is unclear why there is a lack of repair of elastic fibers. We have examined fibroblasts cultured from lung tissue from normal and COPD subjects to determine if the secretory profile explains lack of tissue repair. In this study, fibroblasts were cultured from lung parenchyma of bronchial carcinoma patients with varying degrees of COPD; controls (non-COPD, n=5), mild COPD (GOLD 1, n=5) and moderate-severe COPD (GOLD 2-3, n=12). Measurements were made of proliferation, senescence-associated beta-galactosidase-1, mRNA expression of IL-6, IL-8, MMP-1, tropoelastin and versican, and protein levels for IL-6, IL-8, PGE2, tropoelastin, insoluble elastin, and versican. It was found that GOLD 2-3 fibroblasts proliferated more slowly ($p<0.01$) and had higher levels of senescence-associated beta-galactosidase-1 ($p<0.001$) than controls (non-COPD). GOLD 2-3 fibroblasts showed significant increases in mRNA and/or protein for IL-6, IL-8, MMP-1, PGE2, versican ($p<0.01$) and tropoelastin ($p<0.05$). mRNA expression and/or protein levels of tropoelastin ($p<0.01$), versican ($p<0.02$), IL-6 ($p<0.05$) and IL-8 ($p<0.05$) were negatively correlated with FEV1%. Insoluble elastin was not increased. In summary, fibroblasts from moderate to severe COPD subjects display a secretory phenotype with up-regulation of inflammatory molecules including the matrix proteoglycan versican, and increased soluble, but not insoluble, elastin. Versican inhibits assembly of tropoelastin into insoluble elastin and we conclude that the pro-inflammatory phenotype of COPD fibroblasts it is not compatible with repair elastic fibers.

***Keywords*—**COPD,pulmonary fibroblasts, pro-inflammatory phenotype, versican, elastin

I. Introduction

CHRONIC Obstructive Pulmonary Disease (COPD), characterised by irreversible airflow obstruction in the small airways [1, 2], involves both small airway remodelling and emphysematous changes. In moderate and severe COPD elastic fibers are lost from the alveolar walls, a change thought to lead to weakening and loss of alveolar attachments to small airways and to their subsequent collapse in expiration [3]. The loss of elastic fibers in emphysema has been explained by the protease-antiprotease hypothesis [4], elaborated following the description in 1963 of emphysema due to 1-antitrypsin deficiency [5] and associated loss of inhibition of neutrophil elastase. There are reasons, however, for questioning whether neutrophil elastase and 1-antitrypsin are of central importance in COPD. Inherited deficiency of 1-antitrypsin is uncommon and only accounts for a small proportion of cases of COPD, and reduction of 1-antitrypsin levels in the lung has not been consistently demonstrated in individuals with COPD without 1-antitrypsin deficiency [6].

The majority of research on COPD has focussed on the idea that emphysema can be explained by progressive destruction of the alveolar walls but there are several lines of evidence to suggest that inhibition of repair may be important in the pathogenesis of COPD [7, 8]. Thus when damage occurs as a result of smoking there may be differences in the ability to repair this damage and individuals with impaired repair mechanisms may be more likely to develop COPD. Impaired repair, however, does not appear to be due to the inability to synthesise structural matrix proteins such as elastin and collagen.

Elastin is a long-lived molecule with most elastin deposition occurring early in development with little turnover in adult life [9]. Several experimental studies, however, have reported that matrix proteins, including elastin and collagen, are re-synthesised in emphysematous lungs in animal models [10, 11]. Synthesis of elastin, however, does not result in restoration of physiological function, presumably because functional fibers fail to form [12]. Similarly, investigations on human emphysematous lungs report re-synthesis of matrix proteins, but with changed distribution patterns of collagen and elastin, including clumping of elastin deposits in the free edges of alveolar walls [13, 14].

More recently it has been reported that elastin mRNA expression is significantly increased in lungs with very severe COPD (GOLD 4) compared with non-COPD controls and mild or moderate COPD [15]. In situ hybridization localized this increased elastin expression to the alveolar walls, but neither the elastic fiber content nor desmosine levels were increased per lung volume.

Our recent research also provides support for the idea that loss of repair mechanisms may be important in the development of COPD. The impaired repair appears to be due to the inability to form functional insoluble elastic fibers rather than the lack of synthesis of the elastin precursor tropoelastin. We examined lobectomy lung tissue from patients with bronchial carcinoma and found that whereas elastic fiber content was significantly decreased in patients with mild to moderate COPD [16],

1 Department of Pulmonary Medicine, Zhongshan Hospital, Fudan University, Shanghai, China
2 Department of Pharmacology & Clinical Pharmacology, University of Auckland, New Zealand
3 Department of Pulmonary Medicine, Huadong Hospital, Fudan University, Shanghai, China
4 Department of Anatomy with Radiology, University of Auckland, New Zealand.
*Coresponding Author: Lian Wu, l.wu@auckland.ac.nz

versican, a matrix proteoglycan that mediates inflammatory changes, was increased [17]. This increase may be particularly relevant because versican has been shown to inhibit the assembly of tropoelastin into elastic fibers [18-20], which may explain the reduced capacity of COPD lung to form new elastic fibers despite the ability to synthesise the elastin precursor tropoelastin.

In order to examine more closely this inhibition-of-repair hypothesis, we have cultured pulmonary fibroblasts from the lungs of patients with variable degrees of COPD, and from lungs of individuals with a comparable smoking history but normal lung function, to determine if the synthetic profile of fibroblasts, with respect to elastin synthesis and deposition, and synthesis of versican and inflammatory cytokines, changes with disease progression and explains the inhibition of repair seen in lungs with advanced COPD.

II. Methods

Subjects

Primary fibroblasts were obtained from excised lung tissue collected during surgery for bronchial carcinoma at Auckland Hospital, Auckland, New Zealand. All patients had lung function measured preoperatively and those with a clearly documented history of asthma or bronchodilator reversibility (increase in FEV1 > 10% of predicted normal values) were excluded from the study. Patients with other lung diseases, such as bronchiectasis and interstitial lung disease, were also excluded. Twenty two patients met the criteria for the study and were divided into three groups; control (non COPD), mild COPD (GOLD stage 1) and moderate/severe COPD (GOLD stage 2-3). The study was approved by the Northern X Regional Ethics Committee, Ministry of Health. Written informed consent for permission to use the lung tissue for research was obtained preoperatively.

Cultures of Human Lung Fibroblasts

Fibroblasts were cultured from peripheral pleura-free parenchymal specimens of the resected lobe remote from the tumor. The tissues were immediately transferred into explant culture medium [Dulbecco's Modified Eagle Medium (DMEM), 10% fetal calf serum (FCS), penicillin (100 ng/ml), and streptomycin (100 ng/ml)] (Invitrogen), and then minced with a scalpel (1-2mm2) and transferred into 25cm2 culture dishes for primary culture at 37°C in 5% CO2. Cells were trypsinised when they were confluent and passaged. Cells were evaluated in passage 2 after primary culture to confirm that more than 99% of the cells were fibroblasts with typical fibroblast morphology, positive staining for anti-vimentin antibody (Cell Signaling, US), negative staining for anti-pan cytokeratin antibody (Covance, New Jersey US), and mostly negative staining for anti-αSMA antibody (alpha Smooth Muscle Actin, Sigma-Aldrich, US). Cell free supernanants and RNA were obtained from 48-hour subconfluent passage 3 cultures for further ELISA and PCR analysis.

Proliferation

Proliferation was measured on passage 3 fibroblasts using the AlarmaBlue (AB) assay (Invitrogen, USA) as described previously [21]. Briefly, fibroblasts were seeded at 5,000/well into 96 well plates in serum-free culture medium and AB added at a final concentration of 10%. After six-hour incubation in a humidified atmosphere containing 5% CO2, the %AB reduction, which proved linear to cell number, was measured and recorded as the baseline reading. After additional culture for 24 h in complete culture medium (5% CO2 at 37°C), the %AB reduction was measured again. A proliferation index was calculated as the 24 h reading divided by the baseline reading.

Staining for Senescence-associated β-Galactosidase (SA-β-Gal)

A total of 5,000 fibroblasts (passage 3) were transferred onto glass cover chamber slides (LAB-TEK, Nunc, 0.8 cm2). After culture for 24 h under standardized conditions (37°C, 5 % CO2), staining for SA-β-Gal activity at pH 6.0 was performed using a SA-β-Gal staining kit (Cell Signaling Technologies, Beverly, MA, USA). Cells positive for the blue stain were counted under visible light. Total cell number was determined by counting DAPI stained cells under UV light.

Real-time PCR

Total RNA extraction was performed using Trizol Reagent (Invitrogen Life Technologies, USA) and 1μg of total RNA transcribed using SuperScript® ViLOTM cDNA synthesis kit (Invitrogen Life Technologies, USA) according to the manufacturer's instructions. Real-time PCR was performed using Express SyBR® GreenERTM SuperMix with Premixed ROX (Invitrogen Life Technologies, USA) following the manufacturer's instructions. PCR assays were performed in duplicate on a 7900HT real-time PCR machine (Applied Biosystems, USA) with cycler conditions as follows: incubation for 2 min at 50 °C followed by another incubation step at 95 °C for 10 min, afterwards 15 s at 95 °C and 1 min at 60 °C for 40 cycles. Reaction specificity was evaluated by melting curve analysis, performed by heating the plate from 55 to 95°C and measuring SYBR Green I dissociation from the amplicons. The calculation of threshold cycles (Ct values) and further analysis of these data were performed by Sequence Detector software. The relative mRNA expression of target genes in each sample were quantified and normalized to the GAPDH mRNA levels by the 2-ddCt method [22]. The sequences of each primer pair used for each mRNA analyzed are listed in Table 1.

ELISA

For ELISA analyses, MMP-1 kit from Calbiochem (Calbiochem, USA), PGE2 kit from Pharmaco (Pharmaco Life Science, USA), IL-6 and IL-8 kits from BD (Becton and Dickinson, USA) and versican kit from CUSABio were purchased. The level of protein of interest in cell-free culture supernatants was determined according to the manufacturer's instructions.

Quantification for Elastin

Passage 3 cells were seeded at 50,000cells/well in 6-well plates and cultured for two weeks. Cell-free supernatant was collected for measuring soluble elastin. For insoluble elastin, cell layers were scraped in 0.1N NaOH, sedimented by

centrifugation, and boiled in 0.5mL of 0.1N NaOH for 45 minutes to solubilize all matrix components except elastin. The resulting pellets containing the insoluble elastin were solubilized by boiling in 5.7N HCl for 1hour for further analysis. A Fastin elastin assay kit from Biocolor was used to measure the protein concentration according to the manufacturer's instruction.

Statistics

All statistical analyses were performed using GraphPadPrism 5.0 for Windows. D'Agostino and Pearson omnibus normality test was performed on all data. Data normally distributed were expressed as mean±SD, and one-way analysis of variance followed by Bonferroni post test was performed to determine whether the differences between the groups were statistically significant. Otherwise, data were expressed as median (minimum, maximum), and comparisons were made using the Kruskal-Wallis analysis followed by Dunn's multiple comparison test. Correlation analyses were carried out using Pearson or Spearman methods depending on the normality of the data distribution. Differences were considered significant at the level of $p< 0.05$.

III. Results

Clinical and Demographic Features of the Subjects

Twenty-two patients met the criteria for the study and were divided into three groups according to the results of spirometry: control (non-COPD), mild COPD (GOLD stage 1) and moderate/severe COPD (GOLD stage 2-3) (Table 2). The three groups were similar in age, gender and smoking status but differed significantly in lung function. As expected, the subjects in the moderate/severe COPD group (GOLD stage 2-3) had significantly lower FEV1% predicted and FEV1/FVC% (forced vital capacity %) values compared with non-COPD group and mild COPD group (See Table 2 for details).

Cell Morphology

The primary cultures of lung fibroblasts displayed morphological features typical of fibroblasts and immunostaining demonstrated that >99% of cells were vimentin-positive (Figure 1A) and anti-pan cytokeratin negative and mostly anti-αSMA negative (data not shown). Notably, the slower growing fibroblasts from GOLD 2-3 COPD patients were often less spindle shaped and more flattened and spread than cells from control patients (non-COPD) (Fig 1 B,C), features shown previously to be associated with slower growth and an elastogenic phenotype [23, 24].

Cell Proliferation and Cell Senescence

Proliferation, determined by the AlarmaBlue (AB) assay, was significantly slower in fibroblasts from GOLD 2-3 COPD subjects (1.21±0.22) than from non-COPD subjects (1.65±0.23) ($p<0.01$) (Figure 2A). Cell senescence, determined by β-Galactosidase (SA-β-Gal) staining, was significantly increased in the GOLD 2-3 COPD fibroblasts (32.5% + 6.5%, mean + SD) compared to non-COPD controls (19.5% + 2.3%, mean + SD) ($p<0.001$) and GOLD 1 fibroblasts (19.3% + 1.8%, mean + SD) ($p<0.01$) (Fig 2B).

mRNA and Protein levels

MMP-1 mRNA was significantly ($p=0.01$ and $p=0.02$ respectively) increased in the GOLD 2-3 COPD cultures compared to non-COPD and GOLD 1 COPD (Figure 3). IL-6 and IL-8 mRNA expression levels were significantly ($p<0.01$) raised in the GOLD 2-3 COPD cultures (Fig 4A and 4B) as were the respective protein levels ($p<0.01$ and $p<0.001$) (Fig 4C and 4D). mRNA expression levels of IL-6 and IL-8 were negatively correlated with FEV1 pred% (Spearman r = -0.6316, p=0.004; and Spearman r = -0.626, p=0.003) respectively (data not shown). Secreted levels of IL-6 and IL-8 also negatively correlated with FEV1 % predicted, (Pearson r = -0.6604, p=0.01; and Pearson r = -0.8205, p=0.001) respectively (data not shown).

Levels of PGE2 in supernatants were significantly higher in the GOLD 2-3 COPD fibroblast cultures than in non-COPD ($p<0.05$) cultures (Fig 5). There was a weak but significant relationship between PGE2 and FEV1 % of predicted (Pearson r = -5015, p=0.03) (data not shown).

Elastin precursor mRNA (hnRNA) was significantly ($p<0.05$) increased in fibroblasts from the GOLD 2-3 subjects compared to the non-COPD controls (Fig 6A). Patients with a lower FEV1 % predicted had higher mRNA relative expression than subjects with higher FEV1 % of predicted values (Spearman r = -0.7511, p=0.001) (Fig 6B). Similarly, soluble elastin released into the media was significantly higher in the GOLD 2-3 cultures compared with non-COPD ($p<0.05$) and GOLD 1 cultures ($p<0.05$) (Fig 6C). Soluble elastin level was also negatively related to the FEV1 % of predicted value of patients (Spearman r = -0.7677, p= 0.002) (Fig 6D). There was no difference between groups, however, in the amount of insoluble elastin deposited into the cell layers (Fig 6E), indicating that the increased amount of soluble tropoelastin in the GOLD 2-3 cultures was not incorporated into insoluble elastin. Variation in levels of insoluble elastin between subjects was not correlated with FEV1 % predicted (p=0.5) (data not shown). Elastin binding protein (EBP) mRNA was also significantly increased (p=0.03) in Gold 2-3 cultures (medians of expression index: non-COPD 0.25, GOLD 1 COPD 0.10 and GOLD 2-3 COPD 2.40, p=0.03).

Versican mRNA (Fig 7A) and versican levels measured by ELISA (Fig 7C) were significantly ($p<0.05$) increased in GOLD 2-3 cultures compared to the non-COPD controls. Moreover, versican mRNA expression was strongly negatively correlated with FEV1% predicted (Spearman r = -0.8232, p=0.001) (Fig 7B). A similar correlation was detected for secreted versican (Pearson r = -0.7094, p=0.02) (Fig 7D). Versican production by GOLD 1 fibroblasts was not significantly different from non-COPD fibroblasts, although versican mRNA was slightly non-significantly elevated (Fig 7A). Biglycan mRNA was also increased (medians of expression index: non-COPD 239.1, GOLD 1 COPD 79.8 and GOLD 2-3 COPD 1186, p=0.03) in GOLD 2-3 cultures while the collagen-associated proteoglycan decorin showed a non-significant increase (medians of expression index: non-COPD 1131, GOLD 1 COPD 216.8 and GOLD 2-3 COPD

3446, p>0.05). Collagen–1 mRNA was significantly increased (p=0.02) in GOLD 2-3 cultures (medians of expression index: non-COPD 5374, GOLD 1 COPD 517.3 and GOLD 2-3 COPD 12610, p=0.02).

IV. Discussion

This study demonstrates that fibroblasts derived from the peripheral parenchyma of lungs of patients with moderate to severe COPD (GOLD stages 2-3) have a distinctly different phenotype from fibroblasts cultured from patients with mild COPD (GOLD stage 1) or non COPD. Fibroblasts from the GOLD 2-3 COPD group had slower proliferation rates and increased levels of SA β-Gal compared to fibroblasts from the control and mild COPD groups, but were significantly more metabolically active, synthesizing increased amounts of inflammatory cytokines IL-6 and IL-8 and PGE2, and the pro-inflammatory matrix proteoglycan versican. These results are consistent with the findings from other research groups [25-27]. Synthesis of soluble tropoelastin was also increased. The increases in both versican and tropoelastin were negatively correlated with FEV1 % predicted values across all patients. Collectively these data point to fibroblasts in the alveolar walls lungs with COPD having an active pro-inflammatory secretory profile that is enhanced with deterioration of lung function.

The increased synthesis of soluble elastin indicates that COPD fibroblasts are capable of producing this extracellular component of major importance to alveolar structure and function. Notably, however, the increase in elastin message and in soluble tropoelastin was not matched by an increase in insoluble elastin, necessary for fiber formation. In previous immunohistochemical studies of COPD lung parenchyma we found that elastin content, measured by morphometry, progressively decreases as FEV1 decreases [16] and is associated with a reciprocal and progressive increase in versican [16, 17]. A more recent study has found that fibroblasts cultured from peripheral lung samples from COPD patients show elevated production of versican [25], as found in this current study. The increase in versican in COPD may be particularly relevant as versican inhibits the assembly of tropoelastin into soluble into elastic fibers, both in cell culture and in vivo [18-20]. Thus the elevated production of versican in COPD is consistent with the lack of formation of new elastic fibers in COPD lung, despite fibroblasts to synthesising increased amounts of tropoeolastin.

Versican belongs to the family of large aggregating chondroitin sulphate (CS) proteoglycans located primarily within the extracellular matrix (ECM). CS chains, constitutent to three isoforms of versican (V0, V1, V2), inhibit the assembly of tropoelastin into elastic fibers by displacing elastin binding protein (EBP) from the cell surface. EPB is the receptor that chaperones tropoelastin through the golgi to the external cell membrane [19] and its displacement from the cell surface prevents the transfer of tropoelastin to the microfibrillar scaffold [19]. As a result, fiber formation is disrupted. The increase in EBP mRNA in Gold 2-3 fibroblasts, along with the increase in soluble elastin also indicates that these cells have elastogenic potential that is not fully realised. Notably, mRNA for biglycan, which also contains CS chains, was also increased, and similar to versican inhibits elastic fiber formation [28]. We postulate that the mismatch between levels of soluble and insoluble elastin, seen in this current study, can be explained by the elevated production of CS-containing matrix proteoglycans preventing fiber assembly.

Experimental evidence has shown that impaired elastic fiber assembly, caused by pericellular accumulation of CS proteoglycans is reversible. Treatment of skin fibroblasts that overproduce versican, as occurs in Costello syndrome, with chondroitinase reverses the elastic fiber deficiency [19]. Knockdown of versican production by vascular smooth muscle cells (SMC) through over-expression of versican antisense similarly enhances elastic fiber deposition [20], as does over-expression of the glycosaminoglycan deficient variant of versican, V3 [13]. Cells over-expressing V3 have a significantly lower level of the larger versican variant V1 on the cell surface, where it is attached to hyaluronan, which reduces CS in the pericellular region [23] allowing a longer residence time for EBP [18]. V3, versican antisense, and chain-less mutant biglycan, are also effective in vivo, and have been used to create elastin-rich, versican depleted neointimae [20, 24, 28]. Over-expression of V3, leading to decreased cell-associated chondroitin sulphate, has also been used successfully to restore elastic fiber formation in cultures of skin fibroblasts from Costello Syndrome patients [29].

Thus, findings from the present and previous studies [16, 17] raise a testable hypothesis, namely that repair of the elastin network in lung parenchyma, and possibly restoration or improvement of physiological function, might be achievable by reducing the CS proteoglycan content of alveolar walls. Lowering of versican in vivo might be particularly effective as the mechanical movements of ventilation likely have a role in determining the pattern and placement of elastic fibers during repair. Moreover, increased assembly of the secreted tropoelastin may lead to a decrease in the level of free tropoelastin-derived peptides that are capable of inducing production of elastolytic MMP's [30].

On the other hand, our study also showed that the inflammatory cytokines IL-6 and IL-8 mRNA and protein levels are elevated in fibroblasts from patients with moderate to severe COPD compared to control fibroblasts. IL-6 and IL-8 are regarded to play an important role in the inflammation of COPD. IL-6 acts as a proinflammatory cytokine and is also associated with epithelial apoptosis and injury in COPD [31]. IL-8 is a potent attractant for neutrophils and is partly responsible for the acute exacerbation and disease progression of COPD [32, 33].The increased levels of IL-6 or IL-8 had been reported in sputum [32], exhaled breath condensate [30] and blood [34]. In this study, an increase in the mRNA levels of both IL-6 and IL-8 was found in primary human fibroblasts from moderate-severe COPD patients compared to non-COPD controls. In addition, the levels were significantly and negatively correlated the value of FEV1 % predicted.

These cytokines are also frequently associated with elevated levels of versican [35-37], which is also pro-inflammatory [38-42] and, through Toll-like receptor TLR2, a facilitator of metastasis in lung [38]. It is likely that persistent elevation of these cytokines, along with elevated MMP-1, inhibits reversion of COPD fibroblasts to the non-inflammatory phenotype that would be necessary for effective long term remodelling and

repair to take place. Elevation of PGE2 could also reduce repair responses as it inhibits several fibroblast repair responses, including chemotaxis [43] and proliferation [44, 45]; on the other hand it increases expression and activity of MMP-2 [45]. A further difficulty in activation of effective repair processes may be the expression by COPD fibroblasts of SA-β-Gal, also noted by others for emphysema [46], and thought to indicate premature aging. Telomere length, however, is not changed and any aging appears to be by a telomere independent mechanism [46].

The findings of the present study suggest that a reduction in inflammation and in particular a reduction in CS-containing versican in COPD lung may be an effective strategy for restoration of elastin and the possible repair of emphysematous changes. Increases in the elastin content of blood vessels has been achieved through overexpression of versican antisense [20] and more recently it has been demonstrated that SMC in vivo expressing the CS-depleted versican variant V3, result in increased intimal elastin content, decreased production of CS-containing versican, and reduced macrophage ingress associated with cholesterol induced inflammatory changes [47]. It remains to be determined if similar treatments might be effective in reducing the inflammatory changes associated with COPD and in creating a matrix environment permissive for the assembly of tropoelastin into insoluble fibers. Regardless, the persistence of an inflammatory phenotype in COPD would appear to be a major inhibitor of repair.

ACKNOWLEDGEMENTS

This work was supported by Auckland Medical Research Foundation, Faculty Research Development Fund, and the National Natural Science Foundation of China (No. 81000013) and the Shanghai Leading Academic Discipline Project (No. B115).

Dedication:

This Paper is dedicated to our close friend and mentor Professor Peter Black who died suddenly in January 2010. Peter was instrumental in the conception and design of this study. His death is a huge loss to us personally and to the COPD research community.

REFERENCES

[1] Hogg JC, Macklem PT, Thurlbeck WM. Site and nature of airways obstruction in chronic obstructive lung disease. N Engl J Med 1968; 278; 1355-60.

[2] Hogg JC, Timens W. The pathology of chronic obstructive pulmonary disease. Annu Rev Pathol 2009; 4: 435-459.

[3] Jeffery PK. Remodeling in asthma and chronic obstructive lung disease. Am J Respir Crit Care Med. 2001 Nov 15;164(10 Pt 2):S28-38. Review. PubMed PMID:11734464.

[4] Sharafkhaneh A, Hanania NA, Kim V. Pathogenesis of emphysema: from the bench to the bedside. Proc Am Thorac Soc 2008; 5: 475-477.

[5] Laurell CB, Eriksson S. The electrophoretic alpha-1-globulin pattern in alpha-1-antitrypsin deficiency. Scand J Clin Lab Invest 1963; 15: 132-140.

[6] Stone PJ, Calore JD, McGowan SE, Bernardo J, Snider GL, Franzblau C. Smokers do not have less functional alpha 1-protease inhibitor in their lower respiratory tracts than nonsmokers. Chest. 1983 May;83(5 Suppl):65S-66S. PubMed PMID:6601572.

[7] Holz O, Zühlke I, Jaksztat E, et al. Lung fibroblasts from patients with emphysema show a reduced proliferation rate in culture. Eur Respir J 2004; 24: 575-579.

[8] Togo S, Holz O, Liu X, et al. Lung fibroblast repair functions in patients with chronic obstructive pulmonary disease are altered by multiple mechanisms. Am J Respir Crit Care Med 2008; 178: 248-260.

[9] Shapiro SD, Endicott SK, Province MA, Pierce JA, Campbell EJ. Marked longevity of human lung parenchymal elastic fibers deduced from prevalence of D-aspartate and nuclear weapons related radiocarbon. J Clin Invest 1991; 87: 1828-34.

[10] Snider GL, Lucey EC, Stone PJ. State of the art: Animal models of emphysema. Am Rev Resp Dis 1986, 133:149-169.

[11] Chambers RC and Laurent GJ. The lung. In Extracellular Matrix, Volume 1, Tissue Function. Edited by Comper WD. The Netherlands, Harwood Academic Publishers GmbH; 1996: 378-409.

[12] Morris SM, Stone PJ, Snider GL, Albright T, Franzblau C. Ultrastructural changes in hamster lung four hours to twenty-four days after exposure to elastase. Anat Rec 1981, 201:523-535.

[13] Osman M, Cantor JO, Roffman S, Keller S, Turino GM, Mandl I. Cigarette smoke impairs elastin resynthesis in lungs of hampsters with elastase-induced emphysema. Am Rev Resp Dis 1985, 132:640-643.

[14] Fukuda Y, Masuda Y, and Ishizaki M. Morphogenesis of abnormal elastic fibers in panacinar and centriacinar emphysema. Hum Pathol 1989, 20:652-659.

[15] Deslee G, Woods JC, Moore CM, Liu L, Conradi SH, Milne M, Gierada DS, Pierce J, Patterson A, Lewit RA, Battaile JT, Holtzman MJ, Hogg JC, Pierce RA. Elastin expression in very severe human COPD. Eur Respir J. 2009 Aug;34(2):324-31.

[16] Merrilees MJ, Ching PS, Beaumont B, Hinek A, Wight TN, Black PN. Changes in elastin, elastin binding protein and versican in alveoli in chronic obstructive pulmonary disease. Respir Res. 2008 May 18;9:41.

[17] Black PN, Ching PS, Beaumont B, Ranasinghe S, Taylor G, Merrilees MJ. Changes in elastic fibers in the small airways and alveoli in COPD. Eur Respir J. 2008 May;31(5):998-1004. Epub 2008 Jan 23.

[18] Hinek A, Mecham RP, Keeley F, Rabinovitch M. Impaired elastin fiber assembly related to reduced 67-kD elastin-binding protein in fetal lamb ductus arteriosus and in cultured aortic smooth muscle cells treated with chondroitin sulfate. J Clin Invest. 1991;88:2083-94.

[19] Hinek A, Smith AC, Cutiongco EM, Callahan JW, Gripp KW, Weksberg R. Decreased elastin deposition and high proliferation of fibroblasts from Costello syndrome are related to functional deficiency in the 67-kD elastin-binding protein. Am J Hum Genet. 2000;66:859-72.

[20] Huang R, Merrilees MJ, Braun K, Beaumont B, Lemire J, Clowes AW, Hinek A, Wight TN: Inhibition of versican synthesis by antisense alters smooth muscle cell phenotype and induces elastic fiber formation in vitro and in neointima after vessel injury. Circ Res. 2006;98:370-377.

[21] Al-Nasiry S, Geusens N, Hanssens M, Luyten C, Pijnenborg R. The use of Alamar Blue assay for quantitative analysis of viability, migration and invasion of choriocarcinoma cells. Hum Reprod 2007;22:1304-9.

[22] Fink L, Seeger W, Ermert L, Hänze J, Stahl U, Grimminger F, Kummer W, Bohle RM. Real-time quantitative RT-PCR after laser-assisted cell picking. Nat Med. 1998 Nov;4(11):1329-33. PubMed PMID: 9809560.

[23] Lemire JM, Merrilees MJ, Braun KR, Wight TN. Over-expression of the V3 variant of versican alters arterial smooth muscle cell adhesion, migration, and proliferation in vitro. J Cell Physiol. 2002;190:38-45.

[24] Merrilees MJ, Lemire JM, Fischer JW, Kinsella MG, Braun KR, Clowes AW, Wight TN. Retrovirally mediated over-expression of versican V3 by arterial smooth muscle cells induces tropoelastin synthesis and elastic fiber formation in vitro and in neointima after vascular injury. Circ Res. 2002;90:481-7.

[25] Hallgren O, Nihlberg K, Dahlbäck M, Bjermer L, Eriksson LT, Erjefält JS, Löfdahl CG, Westergren-Thorsson G. Altered fibroblast proteoglycan production in COPD. Respir Res. 2010 May 11;11:55. PubMed PMID: 20459817; PubMed Central PMCID: PMC2886021.

[26] Asano K, Shikama Y, Shibuya Y, Nakajima H, Kanai K, Yamada N, Suzaki H. Suppressive activity of tiotropium bromide on matrix metalloproteinase production from lung fibroblasts in vitro. Int J Chron Obstruct Pulmon Dis. 2008;3(4):781-9. PubMed PMID: 19281093; PubMed Central PMCID: PMC2650607.

[27] Asano K, Shikama Y, Shoji N, Hirano K, Suzaki H, Nakajima H. Tiotropium bromide inhibits TGF-β-induced MMP production from lung fibroblasts by interfering with Smad and MAPK pathways in vitro. Int J Chron Obstruct Pulmon Dis. 2010 Sep 7;5:277-86. PubMed PMID: 20856827; PubMed Central PMCID: PMC2939683.

[28] Jin-Yong Hwang, Pamela Y. Johnson, Kathleen R. Braun, Alexander Hinek, Jens W. Fischer, Kevin D. O'Brien, Alexander W. Clowes,

Mervyn J. Merrilees, Thomas N. Wight. Retrovirally-mediated overexpression of glycosaminoglycan-deficient biglycan in arterial smooth muscle cells Induces tropoelastin synthesis and elastic fiber formation in vitro and in neointima after vascular injury. American Journal of Pathology 2008; 173:1919-1928.

[29] Hinek A, Braun KR, Liu K, Wang Y, Wight T: Retrovirally mediated overexpression of versican V3 reverses impaired elastogenesis and heightened proliferation exhibited by fibroblasts from Costello syndrome and Hurler disease patients. Am J Pathol 2004, 164:119-131.

[30] Maquart F-X, Pasco S, Ramont L, Hornebeck W, Monboisse J-C: An introduction to matrikines: extracellular matrix-derived peptides which regulate cell activity. Implication in tumor invasion. Crit Rev Oncol/Hemat 2004, 49:199-202.

[31] Eddahibi S, Chaouat A, Tu L, Chouaid C, Weitzenblum E, Housset B, et al. Interleukin-6 gene polymorphism confers susceptibility to pulmonary hypertension in chronic obstructive pulmonary disease. Proc. Am. Thorac. Soc. 2006; 3: 475-6.

[32] Keatings VM, Collins PD, Scott DM, Barnes PJ. Differences in interleukin-8 and tumor necrosis factor-alpha in induced sputum from patients with chronic obstructive pulmonary disease or asthma. Am. J. Respir. Crit. Care. Med. 1996; 153: 530-4.

[33] Ko FW, Leung TF, Wong GW, Ngai J, To KW, Ng S, et al. Measurement of tumor necrosis factor-alpha, leukotriene B4, and interleukin 8 in the exhaled breath condensate in patients with acute exacerbations of chronic obstructive pulmonary disease. Int. J. Chron. Obstruct. Pulmon. Dis. 2009; 4: 79-86.

[34] Lee TM, Lin MS, Chang NC. Usefulness of C-reactive protein and interleukin-6 as predictors of outcomes in patients with chronic obstructive pulmonary disease receiving pravastatin. Am. J. Cardiol. 2008; 101: 530-5.

[35] Le Bellego F, Perera H, Plante S, Chakir J, Hamid Q, Ludwig MS. Mechanical strain increases cytokine and chemokine production in bronchial fibroblasts from asthmatic patients. Allergy. 2009 Jan;64(1):32-9. Epub 2008 Dec 12.

[36] Beikler T, Peters U, Prior K, Eisenacher M, Flemmig TF. Gene expression in periodontal tissues following treatment. BMC Med Genomics. 2008 Jul 7;1:30.

[37] Klapperich CM, Bertozzi CR. Global gene expression of cells attached to a tissue engineering scaffold. Biomaterials. 2004 Nov;25(25):5631-41.

[38] Kim S, Takahashi H, Lin W-W, Descargues P, Grivennikov S, Kim Y, Luo J-L, Karin M. Carcinoma-produced factors activate myeloid cells through TRL2 to stimulate metastasis. Nature 2009;547:102-106.

[39] Seidelmann SB, Kuo C, Pleskac N, Molina J, Sayers S, Li R, Zhou J, Johnson P, Braun K, Chan C, Teupser D, Breslow JL, Wight TN, Tall AR, Welch CL. Athsq1 is an atherosclerosis modifier locus with dramatic effects on lesion area and prominent accumulation of versican. Arterioscler Thromb Vasc Biol. 2008;28:2180-6.

[40] Zheng PS, Vais D, Lapierre D, Liang YY, Lee V, Yang BL, Yang BB. PG-M/versican binds to P-selectin glycoprotein ligand-1 and mediates leukocyte aggregation. J Cell Sci. 2004;117:5887-95.

[41] Potter-Perigo S, Johnson PY, Evanko SP, Chan CK, Braun KR, Wilkinson TS, Altman LC, Wight TN. Polyinosine-polycytidylic acid stimulates versican accumulation in the extracellular matrix promoting monocyte adhesion. Am J Respir Cell Mol Biol. 2010;43:109-120.

[42] Evanko SP, Potter-Perigo S, Johnson PY, Wight TN. Organization of hyaluronan and versican in the extracellular matrix of human fibroblasts treated with the viral mimetic Poly I:C. J Histochem Cytochem. 2009;57:1041-1060.

[43] White ES, Atrasz RG, Dickie EG, Aronoff DM, Stambolic V, Mak TW, Moore BB, Peters-Golden M. Prostaglandin E(2) inhibits fibroblast migration by E-prostanoid 2 receptor-mediated increase in PTEN activity. Am J Respir Cell Mol Biol 2005;32:135–141.

[44] Lama V, Moore BB, Christensen P, Toews GB, Peters-Golden M. Prostaglandin E2 synthesis and suppression of fibroblast proliferation by alveolar epithelial cells is cyclooxygenase-2–dependent. Am J Respir Cell Mol Biol 2002;27:752–758.

[45] Liu X, Ostrom RS, Insel PA. cAMP-elevating agents and adenylyl cyclase overexpression promote an antifibrotic phenotype in pulmonary fibroblasts. Am J Physiol Cell Physiol 2004;286:C1089–C1099.

[46] Müller KC, Welker L, Paasch K, Feindt B, Erpenbeck VJ, Hohlfeld JM, Krug N, Nakashima M, Branscheid D, Magnussen H, Jörres RA, Holz O. Lung fibroblasts from patients with emphysema show markers of senescence in vitro. Respir Res. 2006 Feb 21;7:32. PubMed PMID: 16504044; PubMed Central PMCID: PMC1435750.

[47] Merrilees MJ, Beaumont BW, Braun KR, Thomas AC, Kang I, Hinek A, Passi A,Wight TN. Neointima formed by arterial smooth muscle cells expressing versican variant v3 is resistant to lipid and macrophage accumulation. Arterioscler Thromb Vasc Biol. 2011 Jun;31(6):1309-16. Epub 2011 Mar 24. PubMed PMID: 21441139

TABLE I DETAILS OF EACH PRIMER PAIR USED FOR EACH mRNA

	Forward primer (5'-3')	*Reverse primer (5'-3')*
Elastin	TCTGAGGTTCCCATAGGTTAGGG	CTA AGCCTGCAGCAGCTCCT
Collagen-1	GGGCAAGACAGTGATTGAATA	ACGTCGAAGCCGAATTCCT
MMP-1	CCCCAAAAGCGTGTGACAGTA	GGTAGAAGGGATTTGTGCG
Biglycan	TGTGTGTGTGTCTTGTGCTT	AGTGAAAGGGACAGGCGAAG
Decorin	TGGCAACAAAATCAGCAGAG	GCCATTGTCAACAGCAGAGA
Versican 1	CCCAGTGTGGAGGTGGTCTAC	CGCTCAAATCACTCATTCGACGTT
EBP	CCATCCAGACATTACCTGGC	TTGATGGGCCCAGAGGGACA
IL-6	GACAGCCACTCACCTCTTCA	TTCACCAGGCAAGTCTCCTC
IL-8	CTGCGCCAACACAGAAATTATTGTA	TTCACTGGCATCTTCACTGATTCTT

TABLE II CLINICAL AND DEMOGRAPHIC FEATURES OF THE SUBJECTS

	Control (Non-COPD)*	**Mild COPD (stage 1) †**	**Moderate- Severe COPD (stage 2-3)§**	**p-value (one way analysis of variance)**
Gender (M/F)	3/2	3/2	7/5	NS
Age (yrs)	69.5±3.1	62.3±13.1	66.4±9.2	NS
Smoking pack-yrs	30.2±10.1	33.3±15.3	47.1±18.0	NS
FEV1 (L)	2.25±0.39	1.84±0.34	1.47±0.36	0.002
FEV1 % pred	90.2±5.4	91.3±10.3	59.8±9.5	<0.001
FVC (L)	2.971±0.452	2.765±0.621	2.747±0.820	NS
FVC % pred	89.3±10.2	104.3±9.6	78.8±17.3	0.05
FEV1/FVC%	79.3±9.4	65.1±6.2	54.9±8.3	<0.001

Data are presented as mean±SD, and the comparisons made by one-way analysis of variance followed by Bonferroni post test. COPD: chronic obstructive pulmonary disease; M: male; F: female; FEV1: forced expiratory volume in one second; % pred: % predicted; FVC: forced vital capacity; NS: non significant. *: subjects had an FEV1≥ 80%pred and FEV1/FVC>70%. † : subjects had an FEV1≥ 80%pred and FEV1/FVC<70%. §: subjects had an FEV1<80%pred and FEV1/FVC<70%.

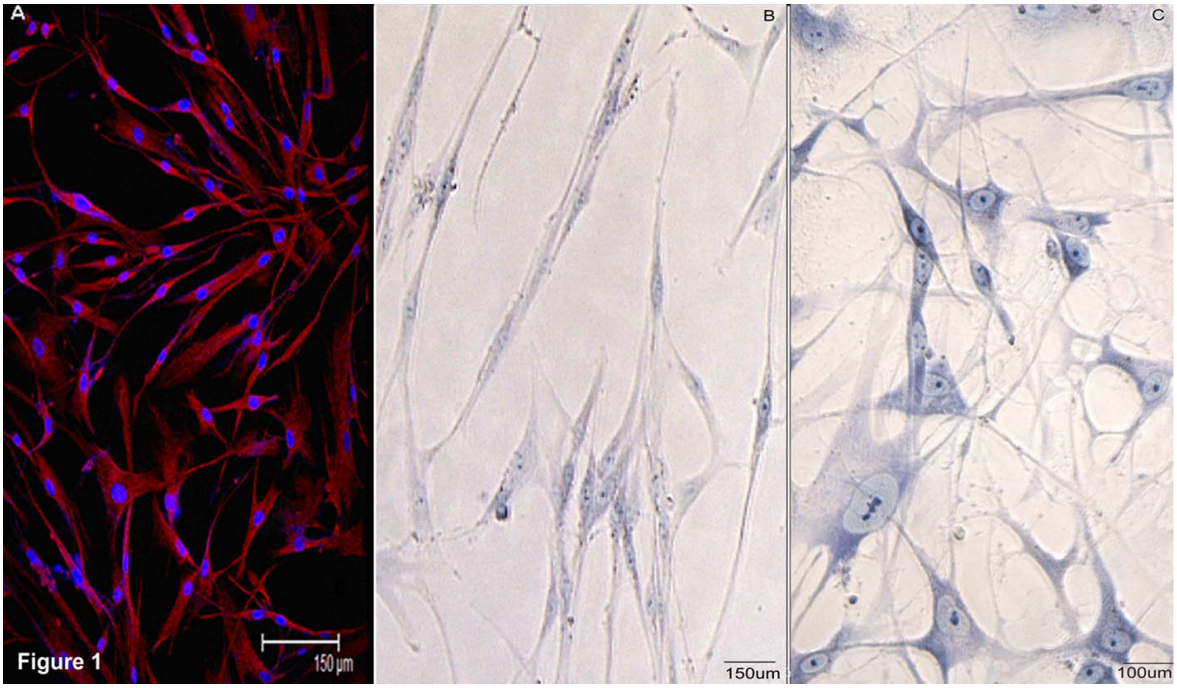

Fig. 1 Cultured fibroblasts from representative non COPD subject and COPD subject.

A Vimentin-stained (red) subconfluent fibroblasts from human lung tissue from non COPD subject. All cells had morphological features typical of fibroblasts. Cell nuclei are stained with Hoechst (blue). **B** Methylene blue stained sparse fibroblasts from non COPD subject showing typical spindle shaped morphology predominant in cultures of fibroblasts cultured from the lungs of non COPD subjects. **C** Methylene blue stained fibroblasts from COPD (GOLD stage 3) subject showing flattened spread morphology frequently seen in cultures of fibroblasts from COPD subjects.

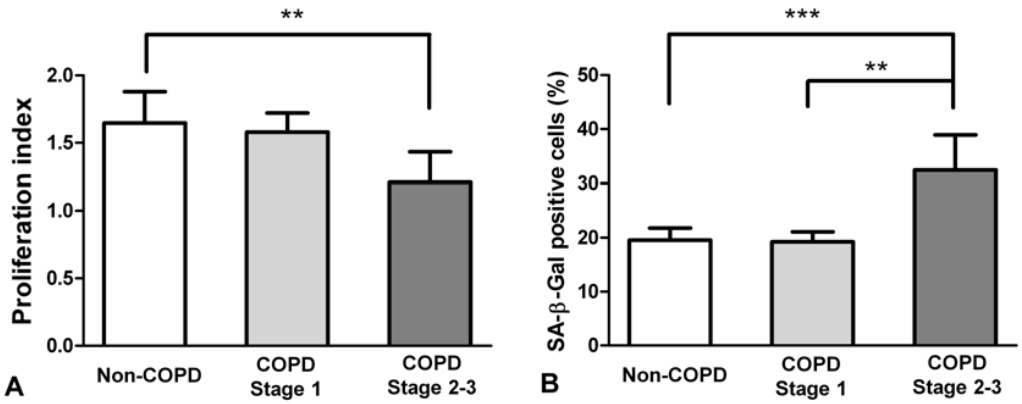

Fig. 2 Reduced proliferation and increased senescence in fibroblasts from moderate and severe COPD subjects.

A: Proliferation index (Alarma Blue assay) showing significantly reduced proliferative capacity of fibroblasts cultured from the COPD Gold Stage 2-3 group compared with the Control and Gold Stage 1 groups. **B**: Significantly increased percentage of SA-β-Gal positive fibroblasts from COPD Gold Stage 2-3 subjects compared to Control and Gold Stage 1 subjects. SA-β-Gal: senescence-associated β-Galactosidase. **: $p<0.01$; ***: $p<0.001$

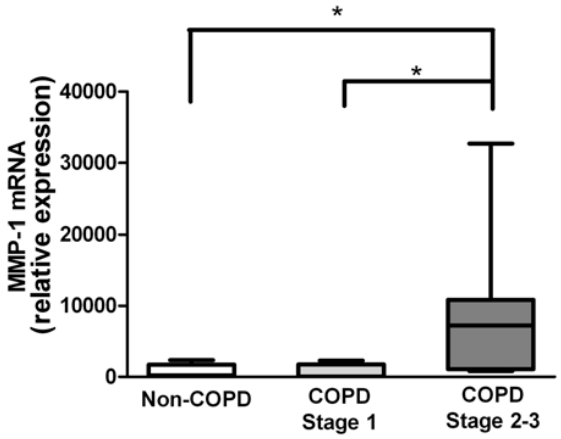

Fig. 3 MMP-1 synthesis.

MMP-1 mRNA expression, detected by real time RT-PCR, relative to expression of GAPDH. Data are expressed as median, upper and lower quartiles (boxed area), and range. *: $p<0.05$.

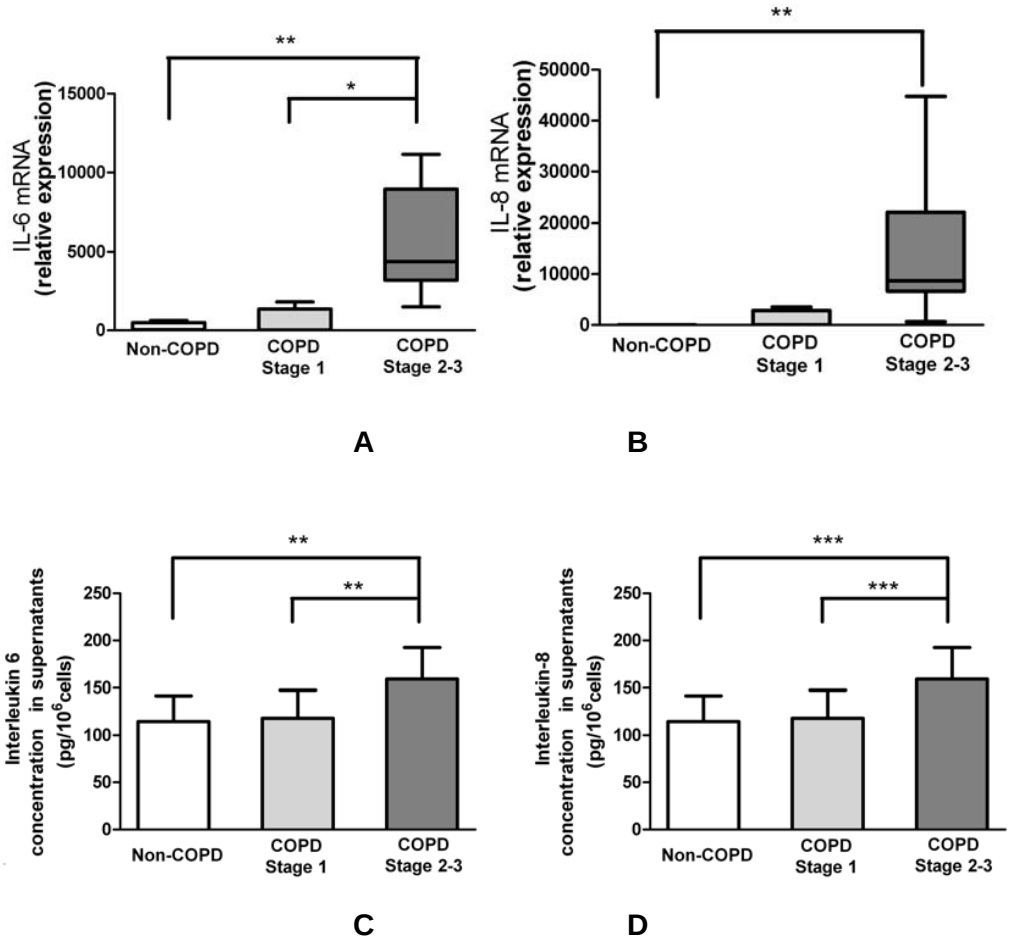

Fig. 4 IL-6 and IL-8 synthesis and secretion.

A and **B** show mRNA expression for IL-6 and IL-8, detected by real-time RT-PCR, relative to expression of GAPDH. Data are expressed as median, upper and lower quartiles (boxed area), and range median (range). **C and D** show IL-6 and IL-8 levels in cell-free supernatants. Data expressed as mean±SD. *: $p<0.05$; **:$p<0.01$; ***: $p<0.001$

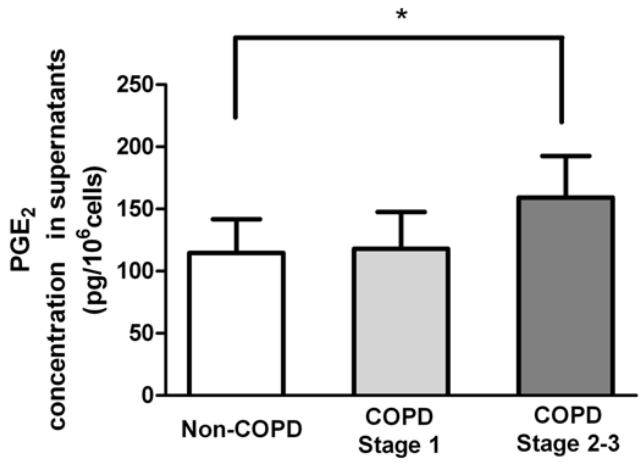

Fig. 5 PGE_2 secretion.

Levels of PGE_2 in supernatant were significant higher in GOLD 2-3 COPD group than in non-COPD and Gold Stage 1 groups. Data are expressed as mean±SD. PGE_2: prostaglandin E_2. *: $p<0.05$.

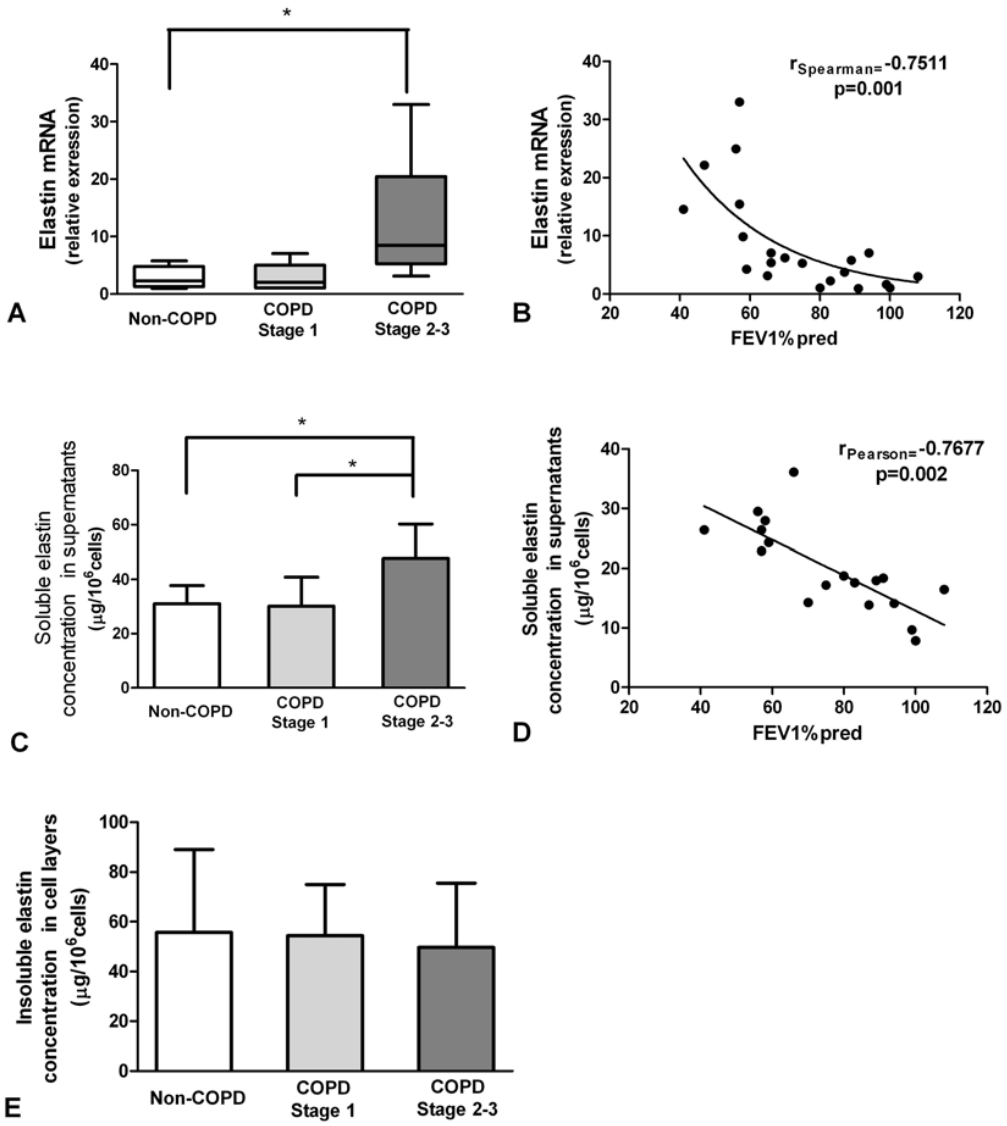

Fig. 6 Synthesis and secretion of elastin.

A Elastin precursor mRNA expression, detected by real time RT-PCR, relative to expression of GAPDH. Data are expressed as median, upper and lower quartiles (boxed area), and range. **B** Correlation between FEV1 % predicted and elastin mRNA relative expression. **C** Levels of soluble elastin in cell-free supernatants. Data are expressed as mean±SD. **D** Correlation between FEV1 % of predicted and tropoelastin levels in the supernatant. **E** Insoluble elastin levels in cell layers. Data are expressed as mean±SD. *: $p<0.05$.

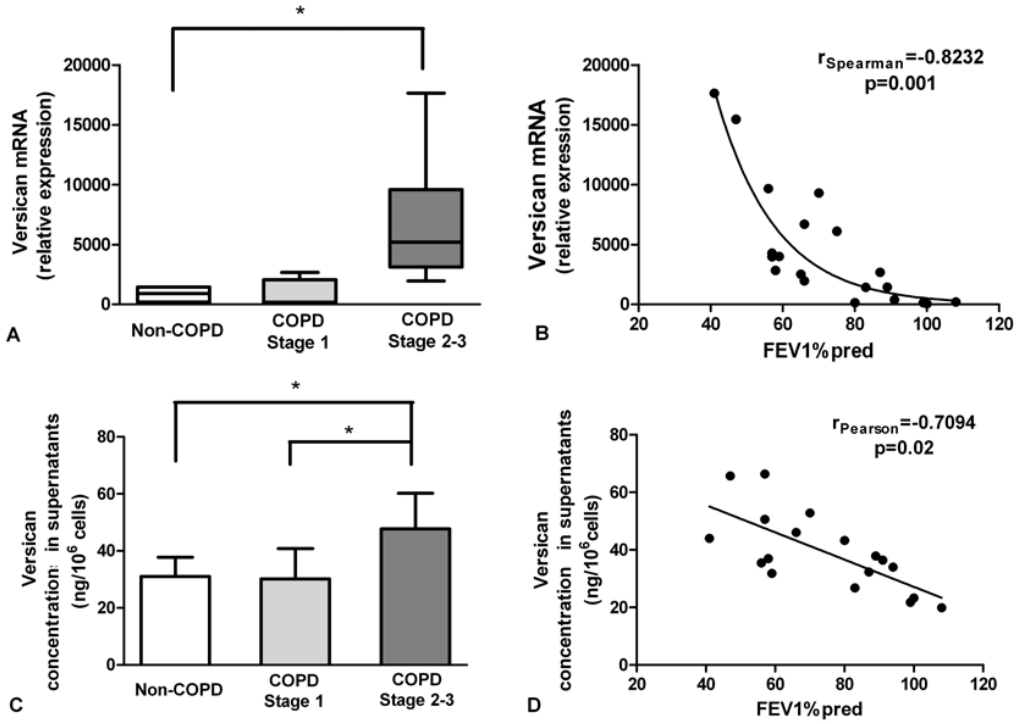

Fig. 7 Synthesis and secretion of versican.

A Versican (V1) mRNA expression, detected by real time RT-PCR, relative to expression of GAPDH. Fibroblasts were cultured for two weeks. Data are expressed as median, upper and lower quartiles (boxed area), and range. **B** Correlation between FEV1 % predicted and versican mRNA relative expression. **C** Versican levels supernatants. Data are expressed as mean±SD. **D** Correlation between FEV1 % predicted and versican levels in supernatants. *, $p<0.05$.